Ultraviolet-Resonance Raman Spectroscopy of the Filamentous Virus Pf3: Interactions of Trp 38 Specific to the Assembled Virion Subunit†

Zai Qing Wen and George J. Thomas, Jr.*

Division of Cell Biology and Biophysics, School of Biological Sciences, University of Missouri−Kansas City, Kansas City, Missouri 64110

Received August 27, 1999

ABSTRACT: The class II filamentous virus Pf3 packages a circular single-stranded DNA genome of ∼6300 nucleotides within a cylindrical capsid constructed from ∼2630 copies of a 44 residue α-helical subunit. The single tryptophan residue (Trp 38) of the capsid subunit is located within a basic C-terminal sequence (...R^+WIK^+AQFF). The local environment of Trp 38 in the native Pf3 assembly has been investigated using 229 nm excited ultraviolet-resonance Raman (UVRR) spectroscopy and fluorescence spectroscopy. Trp 38 exhibits an anomalous UVRR signature in Pf3, including structure-diagnostic Raman bands (763, 1228, 1370, and 1773 cm^{-1}) that are greatly displaced from corresponding Raman markers observed in either detergent-disassembled Pf3, class I filamentous viruses, most globular proteins, or aqueous L-Trp. An unusual and highly quenched fluorescence spectrum is also observed for Trp 38. These distinctive UVRR and fluorescence signatures together reflect interactions of the Trp 38 side chain that are specific to the native Pf3 assembly. The experimental results on Pf3 and supporting spectroscopic data from other proteins of known three-dimensional structure favor a model in which π electrons of the Trp 38 indolyl ring interact specifically with a basic side chain of the subunit C-terminal sequence. Residues Arg 37 and Lys 40 are plausible candidates for the proposed cation−π interaction of Trp 38. The present study suggests that Raman spectroscopy may be a generally useful probe of interactions between the indolyl π-electron system of tryptophan and electropositive groups in proteins and their assemblies.

Bacteriophage Pf3 is a long (∼700 nm) and narrow (∼6 nm) filament infecting strains of *Pseudomonas aeruginosa* that harbor the RP1 plasmid. The Pf3 virion consists of a covalently closed single-stranded (ss)[1] DNA genome of about 6300 nucleotides encased in a sheath comprising about 2630 copies of a 44 residue α-helical subunit (sequence: MQSVITDVTG[10] QLTAVQADIT[20] TIGGAIIVLA[30] AVVLGIRWIK[40] AQFF), plus a few copies of minor proteins at the filament ends. The class II helical architecture of the Pf3 capsid, as defined by fiber X-ray diffraction (*1*), is similar to that of filamentous phage Pf1 but distinct from that of the class I phages fd, f1, and M13 (*2*, *3*). Although assembly pathways of both class I and class II filamentous bacteriophages are of general interest, Pf3 morphogenesis is particularly important because the Pf3 capsid subunit is distinguished by the lack of an N-terminal leader sequence (*4*). The coat subunit of Pf3 represents an attractive model for probing mechanisms of membrane protein insertion and translocation (*5*).

A 3.1 Å model for the arrangement of coat protein subunits in the Pf3 virion has been proposed recently on the basis of fiber X-ray diffraction analysis (*1*). However, the local environments and interactions of subunit side chains, the structure of the packaged ssDNA genome, and the nature of ssDNA−coat protein interactions in the mature assembly remain largely unresolved, owing to both the relatively low resolution of the fiber electron density map and the absence of definitive diffraction from the packaged genome. DNA constitutes only about 14% of the total virion mass. Structural information complementary to that obtained in fiber diffraction analysis can be obtained using various spectroscopic methods, including Raman and ultraviolet-resonance Raman (UVRR) spectroscopy (*6*). In the case of phage fd, polarized Raman microspectroscopy of oriented fibers has been informative of the average inclination angle (16°) of the coat subunit α-helix with respect to the filament axis (*7*). Also, polarized Raman measurements have revealed the spatial orientation of the indolyl ring of the Trp 26 side chain of the coat subunit with respect to the filament axis (*8*). Polarized UVRR spectroscopy of flow-oriented fd in aqueous solution has been used similarly to assess side-chain orientations of Trp 26 (*9*), as well as of Tyr 21 and Tyr 24 (*10*), in the native virion. Implementation of UVRR with appropriately selected excitation wavelengths (*11*) has provided additional structural details on packaged ssDNA and coat protein aromatics in both fd (*12*) and Pf1 (*13*) assemblies. These and related Raman applications enable more accurate modeling of protein−protein and protein−DNA interactions in the viral filaments (*6*).

The most extensively studied filamentous structures (fd, Pf1, and Pf3)—despite rather similar capsid morphologies—differ appreciably in the number and distribution of aromatic side chains in the respective coat proteins. Thus, the 50

† Supported by NIH Grant GM50776.

* To whom correspondence should be addressed.

[1] Abbreviations: CRABPI, cellular retinoic acid binding protein I; rpm, revolutions per minute; SDS, sodium dodecyl sulfate; ss, single-stranded; UVRR, ultraviolet-resonance Raman.

10.1021/bi992018w CCC: $19.00
Published on Web 12/11/1999

residue fd subunit contains the most abundant aromatic amino acid composition, viz., 2 tyrosines (Tyr 21, Tyr 24), 1 tryptophan (Trp 26), and 3 phenylalanines (Phe 11, Phe 42, Phe 45). Conversely, the 46 residue Pf1 subunit contains only 2 aromatics (Tyr 25, Tyr 40), while the 44 residue Pf3 subunit has 1 tryptophan (Trp 38) and 2 phenylalanines (Phe 43, Phe 44). Accordingly, it is expected that details of subunit packing, especially with respect to interactions of aromatic side chains, will differ substantially among the three viral capsids. Because UVRR spectroscopy is a sensitive probe of vibrational dynamics and local environments of aromatic rings, the method is ideally suited to comparative analysis of the local interactions of aromatic amino acid side chains in filamentous virus assemblies. This capability is exploited here to investigate the unique tryptophan residue (Trp 38) of the Pf3 coat subunit and to contrast its environment and interactions within the Pf3 virion with corresponding structural properties of the unique tryptophan residue (Trp 26) of the fd virion.

The present study demonstrates that the UVRR and fluorescence signatures of the Pf3 subunit tryptophan (Trp 38) are unusual and specific to the native virion. Similar spectroscopic markers are not observed in either disassembled Pf3, class I filamentous virions, most globular proteins, or aqueous L-tryptophan (L-Trp). By analogy with proteins of well-characterized three-dimensional structure, we show that the UVRR and fluorescence results can be interpreted in terms of interactions involving the Trp 38 indolyl ring and neighboring basic side chains within the native Pf3 structure. Similar tryptophan interactions have not been identified previously by Raman or UVRR spectroscopy (*14*).

MATERIALS AND METHODS

Sample Preparations. Pf3 and host (*P. aeruginosa*, strain PAO1 bearing the RP1 plasmid), and fd virus and host (*E. coli*, strain Hfr3300), were obtained originally from Dr. Loren A. Day, Public Health Research Institute, New York, NY. Growth media (LB and MS) and L-Trp were purchased from Sigma (St. Louis, MO). D_2O (99.9%) was obtained from Aldrich (Milwaukee, WI).

Pf3 was grown on *P. aeruginosa* (PAO1) in LB medium, and fd was grown on *E. coli* (Hfr3300) in MS medium. Mature viral particles, extruded through the bacterial membrane and into the growth medium, were collected by poly(ethylene glycol) precipitation followed by low-speed centrifugation (10 000 rpm). The virus particles were purified by repeated cycles of centrifugation (60 000 rpm) in 10 mM Tris (pH 7.8) to yield a pellet from which virus solutions were prepared for spectroscopic analyses. Further details of isolation and purification of filamentous viruses for spectroscopic analyses have been described previously (*12, 15*). For UVRR spectroscopy, the virus was resuspended at 0.4 mg/mL in 10 mM Tris (pH 7.8); for fluorescence spectroscopy, Pf3 was diluted to 2.7 μg/mL in the same buffer. Pf3 concentrations were determined by UV absorption spectroscopy assuming a virion extinction coefficient of 4.53 cm^2/mg at 264 nm (*2*). Solutions of L-Trp in H_2O (D_2O) were prepared at ~1 mM, pH (pD) 7.0.

UVRR Spectroscopy. For UVRR spectroscopy, the sample was sealed in a custom-designed cylindrical quartz cell and rotated at 3000 rpm. The spectrum was excited at 229 nm using a continuous-wave, frequency-doubled argon laser (Innova 300 FReD, Coherent Inc., Santa Clara, CA), maintained at a radiant power of 1 mW or less at the sample cell. Raman scattering at 90° was analyzed using a single-grating (2400 g/mm) spectrograph (Spex 750M, Instruments, S. A., Edison, NJ) equipped with a prism predispersive element (McPherson Instruments, Acton, MA) and a liquid-nitrogen-cooled, charge-coupled device detector (Instruments, S. A.). Further details of the design and performance characteristics of the UVRR spectrometer have been described previously (*16*).

The effective spectral resolution was 8 cm^{-1} or less. Raman frequencies were calibrated to ± 1 cm^{-1} using acetonitrile liquid. Each spectrum represents an average of six data collections, each acquired during an exposure of 1 h or less. Interfering cosmic rays and weak Raman scattering of the aqueous buffer and quartz cell were removed as previously described (*16*). Spectral differences were computed to verify that each sample showed no significant time dependence of its UVRR spectrum. Consistent with the previously demonstrated characteristics of the UVRR spectrometer design (*16*), no sample photodecomposition occurred during the data collection protocols. Sample integrity was also confirmed following UVRR data collections by UV absorption spectroscopy.

Fluorescence Spectroscopy. Fluorescence emission spectra were obtained on solutions of native Pf3 at 2.7 μg/mL in 10 mM Tris buffer (pH 7.8) and on disassembled Pf3 at 2.7 μg/mL in 50 mM SDS. Data were collected on a Bowman Series 2 fluorescence spectrometer (SLM Instruments, Urbana, IL) using 295 nm excitation. The bandwidth of excitation and emission slits was 2 nm.

Table 1: Raman Markers of L-Trp and the Subunit Indolyl Ring in Filamentous Viruses fd and Pf3[a]

L-Trp	Trp 26 in fd	Trp 38 in Pf3	modes[b]
757 (754)	757 (754)	763 (759)	*W18*
878 (860)	876 (857)	874 (863)	*W17*
1010	1010	1010	*W16*
1238 (1245)	1238 (1245)	1228 (1234)	*W10*
1340	1340	1340	*W7*
1358 (1354)	1360 (1357)	1370 (1360)	*W7*
1460	1460	1460	*W5*
1550	1560	1546	*W3*
1618 (1613)	1616	1620 (1616)	*W1*
1767 (1764)	1767 (1764)	1773 (1769)	*W18 + W16*

[a] Data are from 229 nm excited UVRR spectra of H_2O (D_2O) solutions. Raman band frequencies are in cm^{-1} units. [b] Nomenclature of reference *21*.

RESULTS

Raman Band Assignments for Pf3. An assignment scheme was proposed previously for Raman bands of several filamentous viruses, including Pf3 (*15*). The earlier Pf3 assignment scheme has been refined on the basis of more recent UVRR and off-resonance Raman studies of viral constituents (*11*), the class I fd virion (*12*), the class II Pf1 virion (*13*), and single-site mutants and residue-specific ^2H and ^{13}C isotopomers of fd (*12, 17*−*20*). Accordingly, Raman bands in the 229 nm UVRR spectrum of Pf3 are assigned definitively as shown in Table 1. (A comprehensive tabulation of assignments, including bands observed in both off-

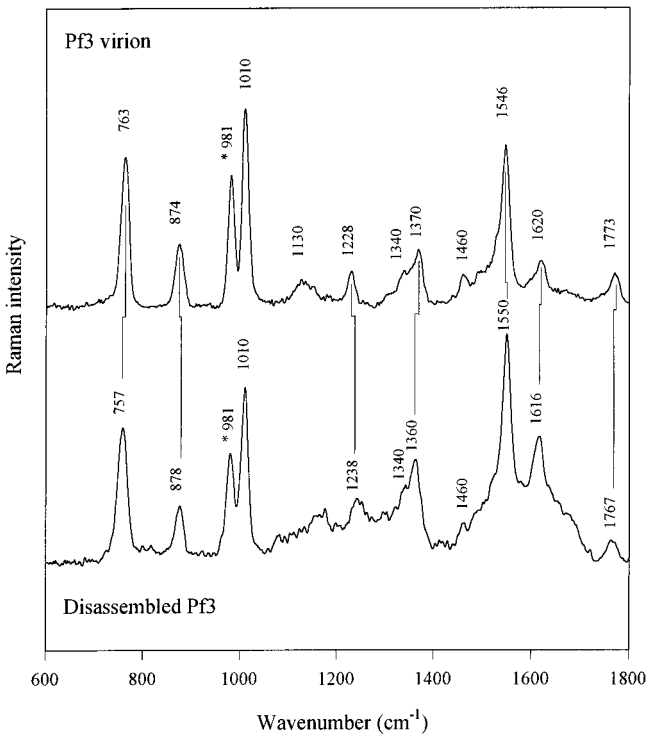

FIGURE 1: UVRR spectra of the native Pf3 virion at 0.4 mg/mL in 10 mM Tris, pH 7.8 (top), and of disassembled Pf3 at ~0.5 mg/mL in 50 mM SDS, pH 7.8. Spectra were excited at 229 nm with a laser power of ~1 mW.

resonance Raman and 257 nm excited UVRR spectra of Pf3, is available upon request from the authors.)

Comparison of UVRR Signatures of the Pf3 Assembly and Disassembled Pf3. The 229 nm UVRR spectrum of a tryptophan-containing protein is expected to be dominated by Raman bands associated with vibrational modes of the indolyl ring(s) (*11, 21*). This is demonstrated for Pf3 in Table 1. To ascertain whether Raman markers of the unique tryptophan (Trp 38) of the Pf3 coat subunit are affected by the state of assembly, we compared the 229 nm UVRR spectrum of the native Pf3 virion with corresponding data from Pf3 disassembled in 50 mM sodium dodecyl sulfate (SDS) solution, as shown in Figure 1. In SDS, the coat subunits are solubilized within detergent micelles (*22*). The data of Figure 1 demonstrate a dramatic change in the local environment of the Trp 38 indolyl ring with virion disassembly. The indolyl normal mode designations and corresponding wavenumber shifts attendant with this assembly → disassembly reaction are as follows: *W18* (763 → 757 cm^{-1}), *W17* (874 → 878 cm^{-1}), *W10* (1228 → 1238 cm^{-1}), *W7* (1370 → 1360 cm^{-1}), *W3* (1546 → 1550 cm^{-1}), *W1* (1620 → 1616 cm^{-1}), and *W18* + *W16* (1773 → 1767 cm^{-1}). To interpret these results, we have examined tryptophan Raman markers in a number of additional proteins and model systems, as described in the following sections.

Raman Markers of Trp 38 Indicate an Unusual Indolyl Environment in the Pf3 Assembly. The Trp 38 Raman markers observed for the disassembled Pf3 subunit (Figure 1, bottom trace) are typical and consistent with UVRR and off-resonance Raman data obtained on many proteins (*14, 23, 24*). Conversely, the Trp 38 Raman markers of the native Pf3 assembly (Figure 1, top trace) are *anomalous*. Collectively, the Raman bands at 763, 874, 1228, 1370, 1546, 1620, and 1773 cm^{-1} represent an unusual indolyl ring environment, evidently specific to the architecture of the Pf3 virion. Figure 2 confirms further that this indolyl environment is not encountered for the Trp 26 side chain of the fd coat subunit. The results of Figure 2 are corroborated by off-resonance Raman signatures of Pf3 and fd (*15, 18, 25*). Thus, although the tubular capsids of both Pf3 and fd are assembled from several thousand copies of a small α-helical subunit, each containing a single tryptophan residue per subunit, the pattern of anomalous tryptophan Raman markers is observed only for Pf3. Indeed, the Trp 26 Raman markers of fd are similar to those observed for aqueous L-Trp, as shown in the bottom trace of each panel of Figure 2. These results are compiled in Table 1.

Fluorescence of Trp 38 Confirms an Unusual Indolyl Ring Environment in Pf3. Figure 3 compares fluorescence emission spectra of Trp 38 in the native Pf3 assembly and in detergent-disassembled Pf3 (50 mM SDS solution). The results show that disassembly generates both an enormous increase (~80%) in the fluorescence peak intensity and a substantial red shift (~10 nm) in the wavelength of maximum emission (λ_{max}). For disassembled Pf3, we find $\lambda_{max} = 342$ nm, which is diagnostic of an indolyl environment that is moderately hydrophobic compared with the amino acid L-Trp in H_2O ($\lambda_{max} \cong 353$ nm), yet not as strongly hydrophobic as that of the assembled virion ($\lambda_{max} = 332$ nm) (*26*). Surprisingly, however, the Trp 38 fluorescence is very strongly quenched in the virion assembly. The fluorescence and Raman data are consistent in demonstrating an unusual environment for Trp 38 in the Pf3 assembly.

Side-Chain Conformation and Nature of the Local Environment of Trp 38 in Pf3. The structural significance of the extraordinary Raman markers and fluorescence characteristics of Trp 38 in the Pf3 assembly can be inferred from examination of previously established spectral correlations and available high-resolution protein structures (*24, 26*−*28*). Thus, the Raman marker at 1546 cm^{-1} (indolyl mode *W3*) indicates that the Trp 38 side-chain torsion $\chi^{2,1}$ (defined by atoms $C^{\delta 1}$-C^{γ}-C^{β}-C^{α}) (*29*) has a magnitude of ~85° in the native Pf3 assembly. On the other hand, for Trp 26 of fd, the *W3* Raman marker occurs at 1560 cm^{-1}, indicating $|\chi^{2,1}| \cong 120°$ in the native fd assembly (*25*). Additionally, for disassembled Pf3, we find *W3* = 1550 cm^{-1} (Figure 1, bottom trace), which corresponds to $|\chi^{2,1}| \cong 90°$. Thus, the very low value (85°) observed for $|\chi^{2,1}|$ in Pf3 reflects a Trp 38 side-chain conformation that is specific to the native virion. The present experimental value is close to the lower limit sterically allowed in proteins (*30*) and differs substantially from the value of 142° proposed for $\chi^{2,1}$ on the basis of model building and fiber X-ray diffraction analysis of Pf3 (Protein Data Bank entry 1IFP) (*1*).

The Pf3 Raman marker at 874 ± 1 cm^{-1} (indolyl mode *W17*, Table 1) identifies a relatively strong hydrogen bond involving the N1H donor of Trp 38 (*24*). The strength of N1H hydrogen bonding decreases appreciably with Pf3 disassembly, as evidenced by the significantly higher wavenumber value (878 cm^{-1}) of *W17* in disassembled subunits (*24*). The N1H hydrogen bond of Trp 26 in the fd assembly (*W17* mode at 876 cm^{-1}) is weaker than that of Trp 38 in the Pf3 assembly, but not as weak as that in disassembled

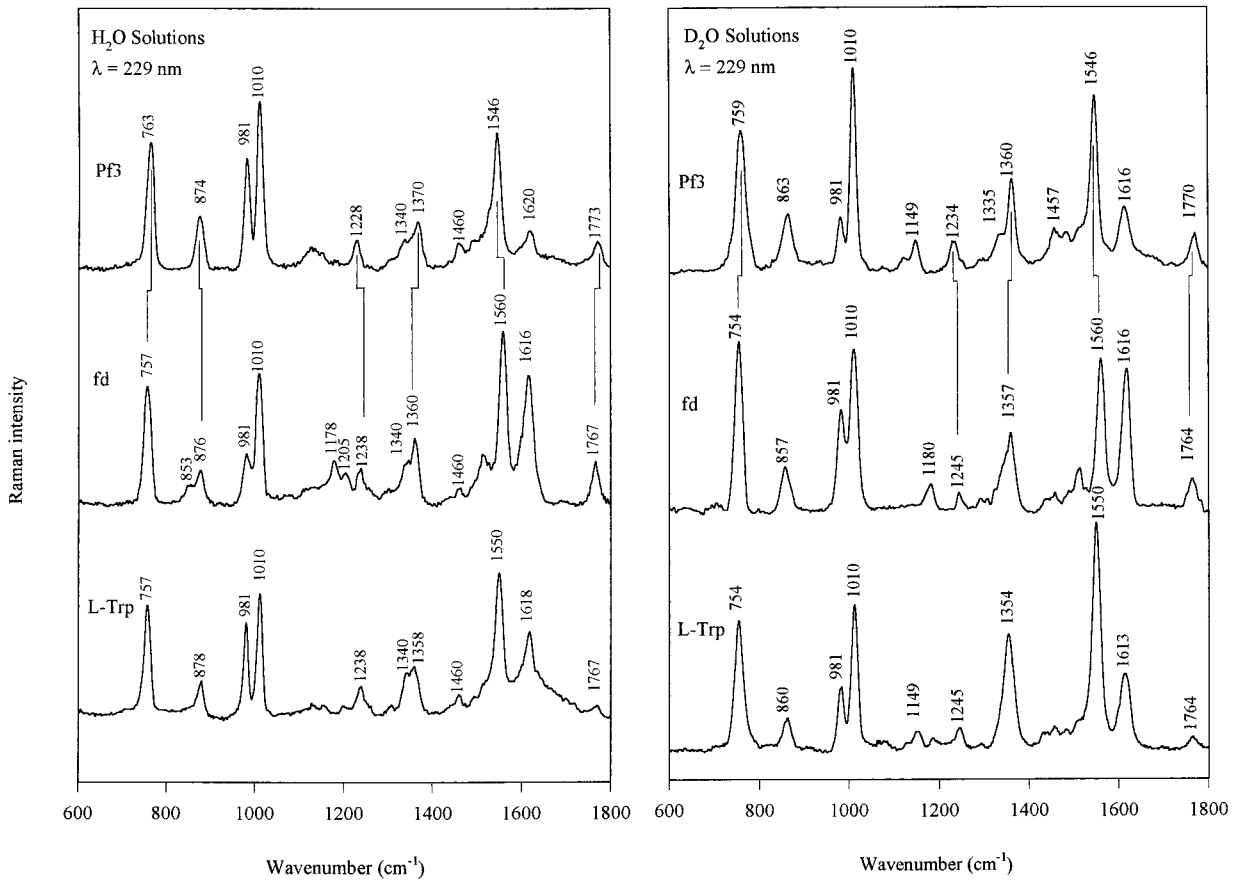

FIGURE 2: UVRR spectra of H_2O (left panel) and D_2O solutions (right panel) of Pf3 (top), fd (middle), and L-Trp (bottom). Sample concentrations: Pf3 and fd, 0.5 mg/mL; L-Trp, 0.39 mM. Spectra were excited at 229 nm with a laser power of ~1 mW.

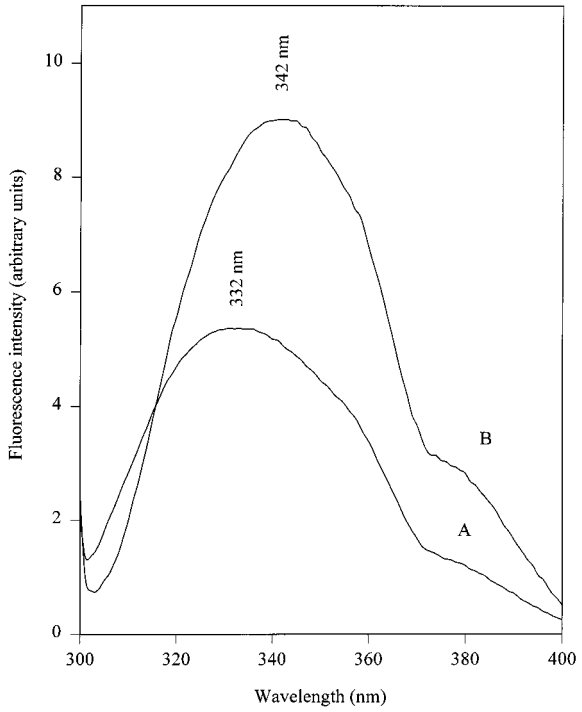

FIGURE 3: Fluorescence spectra excited at 295 nm of (A) Pf3 virus at 2.7 μg/mL in 10 mM Tris, pH 7.8, and (B) disassembled Pf3 at 2.7 μg/mL in 50 mM SDS, pH 7.8.

Pf3. We conclude that the strong N1H hydrogen-bonding state of Trp 38 in Pf3 is also determined by and specific to the assembled Pf3 virion.

The most remarkable features of the UVRR signature of Trp 38 in the Pf3 assembly are the following four Raman bands, all of which originate from vibrations localized within the indolyl ring moiety: 763 (*W18*), 1228 (*W10*), 1370 (*W7*), and 1773 cm^{-1} (*W18* + *W16*). Ordinarily, these Raman markers occur (to within ±1 or 2 cm^{-1}) at 757, 1238, 1360, and 1767 cm^{-1}, respectively (*14*, *23*, *24*), as in fact observed for aqueous L-Trp as well as for Trp 26 of fd (Table 1) and most globular proteins. Corresponding data for D_2O solutions of Pf3, fd, and L-Trp (Table 1) confirm the Pf3 anomaly. In accordance with the above-noted *W3* and *W17* modes, the *W18*, *W10*, *W7*, and *W18* + *W16* modes all shift in the direction expected of canonical tryptophan markers upon virion disassembly in 50 mM SDS (Figure 1).

DISCUSSION

Structural Significance of the Raman and Fluorescence Results. The extraordinary Raman and fluorescence characteristics of Trp 38 are proposed as indicative of an indolyl electronic interaction that is specific to the native Pf3 architecture. This indolyl interaction could result from either *intra*subunit or *inter*subunit contacts, or from a combination of both. The data of Figure 1 demonstrate that the anomalous Trp 38 Raman markers are absent from disassembled subunits, which implies that an intrasubunit contact alone is not sufficient to generate the unusual spectroscopic properties. However, an intrasubunit contact may be imposed by the architecture of the assembled virion. Consistent with this view is the fact that the off-resonance Raman spectrum of a C-terminal nonapeptide fragment of the Pf3 subunit (IR-

Table 2: Raman Markers of the Indolyl Ring (Skatole) in Various Solutions[a]

cyclohexane	acetonitrile	dioxane	H_2O	mode[b]
759	757	757	757	*W18*
880	878	878	878	*W17*
1010	1010	1010	1010	*W16*
1235	1238	—	1238	*W10*
1556	1556	1556	1556	*W3*
1617	1617	1618	1618	*W1*

[a] Data are from 229 nm excited UVRR spectra of skatole solutions (0.5 mM) in the indicated solvents. Raman band frequencies are in cm^{-1} units. [b] Nomenclature of reference *21*.

WIKAQFF) exhibits a completely normal tryptophan Raman signature (*31*).

To further elucidate the nature of the putative Trp 38 interaction in Pf3, we examined databases of other protein structures and tryptophan Raman markers for evidence of similar characteristics. Available data suggest that the Trp 38 Raman markers of Pf3 cannot be accounted for by specific dipolar interaction of the indolyl N1H group or by nonspecific changes in the polarity of the local indolyl ring environment (*12, 14, 24, 27, 32*), such as those associated with solvation effects. Table 2 demonstrates, for example, that the UVRR markers of skatole, a tryptophanyl model compound, are not appreciably perturbed by solvents of greatly differing hydrophobicity and hydrogen-bonding capability (acetonitrile, dioxane, cyclohexane, and water). Also, because the stacking of neighboring indolyl rings with one another or with other aromatics does not perturb the wavenumber values of tryptophan Raman markers in other proteins and in nucleoprotein assemblies (*12*), such interactions are considered unlikely sources of the anomalous Trp 38 Raman markers of Pf3. On the other hand, specific and relatively strong interaction of an electropositive group with the indolyl π-electron system of tryptophan (*33*) could, as documented below, explain the Raman perturbations observed for Pf3. The unusual fluorescence attributes of Trp 38—i.e., very strong quenching and a blue-shift of λ_{max}—also appear to be consistent with specific interaction between the indolyl π-electron system and an electropositive group (*28, 34*).

The Indolyl π-Electron System of Trp 38 as a Putative Acceptor of Cation−π Interaction. Noncovalent attraction between an electropositive group and an aromatic ring, which is referred to as cation$-\pi$ interaction (*33, 35*), is recognized as a potentially significant source of stabilization of proteins and their assemblies. Such attractions are presumed dependent upon the quadrupole moment of the aromatic acceptor system and can involve electropositive donors for which the positive charge is either highly localized (metal cations) or relatively delocalized (lysyl, arginyl, and quaternary ammonium substituents) (*33, 36*). Polarization of the aromatic π-electrons, which is a characteristic of such interactions (*37*), could perturb significantly the vibrational frequencies of the aromatic ring system. Accordingly, cation$-\pi$ interaction should be detectable in Raman and UVRR spectra as an unusual pattern of marker bands. In the case of the indolyl ring, normal modes representing nonsymmetrical ring stretching and ring skeletal bending vibrations, such as *W18*, *W10*, and *W7* (*27*), are among those expected to be sensitive to cation$-\pi$ interaction. The observed UVRR markers of Pf3 (Table 1), as well as previously reported off-resonance Raman markers of this virus (*15*), are proposed as consistent with cation$-\pi$ interaction of Trp 38 in the virion assembly. The observed fluorescence blue-shift and quenching characteristics are also consistent with cation$-\pi$ interaction. The putative electropositive donor to the indolyl π acceptor resides presumably in a basic side chain of the same or a neighboring coat subunit (*33, 36*).

Several lines of evidence support the proposal that the anomalous spectroscopic properties of Trp 38 are due to indolyl interaction with a cationic donor. First, Trp 38 is located between two basic side chains, Arg 37 and Lys 40, either of which could be positioned for favorable intrasubunit cation$-\pi$ interaction. Such an interaction would not conflict with the fiber diffraction-based class II symmetry of Pf3 (*1*). Reorientation of the indolyl ring of Trp 38 through adjustments in side-chain torsion χ^1, while retaining $|\chi^{2,1}| \cong 85°$, might also facilitate favorable cation$-\pi$ interactions at the intersubunit level.

Second, in a recent UVRR study of *Yersinia* protein tyrosine phosphatase (PTPase), an anomalous *W7* marker (1370 cm^{-1}) was reported for Trp 354 (*38*). Although no explanation was given for this *W7* band, it is identical to the *W7* marker of Trp 38 (Table 1) and suggests a similar indolyl interaction. The published UVRR spectrum of *Yersinia* PTPase (*38*) also shows an anomalous *W10* marker (1228 cm^{-1}) identical to the corresponding mode of Trp 38 (Table 1). Interestingly, the X-ray crystal structure of *Yersinia* PTPase (*39, 40*) permits contact between the indolyl ring of Trp 354 and the guanidinium group of Arg 409, which supports the notion of cation$-\pi$ interaction as the basis for the anomalous *W7* and *W10* markers. The data imply that Trp 354 of *Yersinia* PTPase, like Trp 38 of Pf3, is an example of indolyl cation$-\pi$ interaction.

Third, the dramatic increase (~80%) in fluorescence intensity and attendant red-shift of λ_{max} observed for disassembled Pf3 subunits (Figure 3) are not unprecedented. Similar fluorescence effects have been reported for at least one of the three tryptophans (Trp 109) of the *E. coli* cellular retinoic acid binding protein I (CRABPI) (*28*). The unusual Trp 109 fluorescence signature of CRABPI has been attributed to cation$-\pi$ interaction (*28*), consistent with the X-ray crystal structure of this protein (*34*). In CRABPI, Arg 111 furnishes the prospective cation donor group. Although Raman markers of CRABPI have not yet been reported, the similar tryptophan fluorescence characteristics of CRABPI and Pf3 coat protein suggest similar tryptophan interactions. Similar tryptophan Raman markers are anticipated. It will be of interest to examine the tryptophan Raman signature of CRABPI.

Finally, it is instructive to compare the UVRR signature of Pf3 with Raman spectra of previously studied filamentous viruses (*15*). In each of the class I filaments (fd, If1, and IKe), the single tryptophan residue per subunit (Trp 26, Trp 27, and Trp 29, respectively) is located within an extended hydrophobic sequence, which constitutes part of the intersubunit packing domain in the native class I assembly. As expected, each generates a "canonical" pattern of tryptophan Raman markers. Conversely, in the tryptophan-containing class II filamentous viruses, Pf3 and Xf, the single Trp per coat subunit (Trp 38 of Pf3 and Trp 39 of Xf) is located within the basic C-terminal sequence, where it is flanked by

arginine and lysine. In the case of Xf, the subunit C-terminal sequence is even richer in basic side chains (Lys 35, Lys 38, Arg 41, Arg 42) than is that of Pf3 (Arg 37, Lys 40). Remarkably, Trp 39 of Xf also exhibits the anomalous pattern of indolyl Raman markers identified here for Pf3 (*15*). Thus, modes *W18* and *W7* occur in Xf at 765 and 1370 cm^{-1}, i.e., at wavenumber values virtually identical to the corresponding anomalous Raman markers of Pf3 (Table 1). All of the foregoing observations are consistent with a basic side chain (arginine or lysine) as the cation donor in the proposed cation$-\pi$ interaction of Trp 38.

Implications for Mechanisms of Filamentous Virus Assembly. Both class I (fd, If1, IKe) and class II (Pf1, Pf3, Xf) filamentous viruses exhibit extraordinary stability to extremes of temperature, pH, and ionic strength, as well as many other similarities at the level of subunit structure and organization (*15*, *41*−*44*). These similarities have been suggested as evidence that intersubunit interactions are relatively nonspecific and virtually the same in the two assembly classes, and further that the two different classes of virion symmetry are not due to two different sets of specific protein/protein interactions (*1*). However, the present and previous spectroscopic results imply that tryptophan environments and interactions in the well-studied Trp-containing filamentous viruses (fd, If1, IKe, Pf3, and Xf) segregate in rather strict accordance with symmetry class. It is also interesting to note that the coat subunit of the class II virion Pf1, although lacking tryptophan, does contain within its C-terminal sequence an aromatic ring (Tyr 40) that is within one helical turn of a basic side chain (Arg 44). Conceivably, Tyr 40 of Pf1 may fulfill a structure-stabilizing role (i.e., cation$-\pi$ interaction) analogous to that proposed for Trp 38 in Pf3 and Trp 39 in Xf.

Recent UVRR results (*13*) show also that the organization of packaged DNA in the class II Pf1 virion differs fundamentally from that of DNA in the class I fd virion, notably in strength of hydrogen bonding of base exocyclic groups, stacking of specific purines and pyrimidines, and conformations of deoxynucleoside furanose moieties. The spectroscopic results favor diversity in subunit/subunit and subunit/DNA interactions of class I and class II particles and in our view leave open the question of molecular specificity in their assembly.

CONCLUSIONS

Raman and fluorescence spectroscopic studies of native Pf3, disassembled Pf3, and tryptophan model systems provide a body of experimental evidence indicating an interaction of the indolyl ring of Trp 38 of the Pf3 coat subunit that is unusual and specific to the native assembly. Comparison with previously reported X-ray and spectroscopic studies of tryptophan-containing proteins suggests that the indolyl moiety of Trp 38 may be involved in an assembly-specific cation$-\pi$ interaction. Although the interacting cationic group is not identified in the present experiments, plausible candidates are Arg 37 and Lys 40, both of which are located in the same C-terminal region of the subunit sequence. The proposed cation$-\pi$ interaction is consistent with general features of Pf3 virion architecture (*1*) and with the types of stabilizing cation$-\pi$ interactions identified in other protein assemblies (*36*, *45*).

The indolyl $C^{\delta 1}$-C^{γ}-C^{β}-C^{α} torsion, $|\chi^{2,1}|$, determined by UVRR for Trp 38 in Pf3 is $85 \pm 2°$. Previous off-resonance Raman spectra of Pf3 also indicate that $|\chi^{2,1}|$ is close to 85° in the native virion (*15*). This experimental value is within the range (80−113°) of the vast majority of tryptophans in the protein residue rotamer library (*30*). A polarized Raman investigation of oriented Pf3 fibers (M. Tsuboi, K. Nakamura, S. A. Overman, A. Rodriguez-Casado, and G. J. Thomas, Jr., in preparation) indicates further that the Trp 38 indolyl ring of the Pf3 coat subunit is tilted at about 45° to the virion axis. These findings differ significantly from the orientation proposed from fiber X-ray diffraction and model building studies (*1*), wherein $\chi^{2,1} \sim 142°$, situating the indolyl ring close to perpendicular to the virion axis.

The UVRR, Raman, and polarized Raman results together indicate the importance of experimentally based constraints for accurate modeling of filamentous assemblies. The present results should facilitate such modeling and may also help to identify additional intra- and intermolecular interactions in the native structure.

Cation$-\pi$ interactions in proteins have been identified previously on the basis of structures determined by X-ray crystallography (*36*). Fluorescence spectroscopic evidence consistent with cation$-\pi$ interactions has been reported in a few cases (*28*, *46*). Up to the present, however, vibrational spectroscopic markers of cation$-\pi$ interaction have not been identified. The present study suggests that tryptophan-related cation$-\pi$ interactions in proteins are characterized by a distinctive Raman signature, specifically by prominent markers at 763, 1228, 1370, and 1773 cm^{-1} in UVRR spectra. Evidence has been presented that at least two of these markers—at 763 and 1370 cm^{-1}—should also be prominent in off-resonance Raman spectra. Thus, Raman and UVRR may be generally useful probes of cation$-\pi$ interactions of tryptophan residues in proteins and nucleoprotein assemblies.

ACKNOWLEDGMENT

We thank Drs. Roman Tuma, Stacy Overman, James Benevides, and Masamichi Tsuboi for helpful discussions. Support of this research (part LXVII in the series Structural Studies of Viruses by Raman Spectroscopy) by the National Institutes of Health is gratefully acknowledged.

REFERENCES

1. Welsh, L. C., Symmons, M. F., Sturtevant, J. M., Marvin, D. A., and Perham, R. N. (1998) *J. Mol. Biol. 283*, 155−177.
2. Day, L. A., Marzec, C. J., Reisberg, S. A., and Casadevall, A. (1988) *Annu. Rev. Biophys. Biophys. Chem. 17*, 509−539.
3. Makowski, L., and Russell, M. (1997) in *Structural Biology of Viruses* (Chiu, W., Burnett, R. M., and Garcea, R. L., Eds.) pp 352−380, Oxford University Press, New York.
4. Kuhn, A., and Troschel, D. (1992) in *Membrane Biogenesis and Protein Targeting* (Neupert, W., and Lill, R., Eds.) pp 34−47, Elsevier, Amsterdam.
5. Kiefer, D., Hu, X., Dalbey, R., and Kuhn, A. (1997) *EMBO J. 16*, 2197−2204.
6. Thomas, G. J., Jr. (1999) *Annu. Rev. Biophys. Biomol. Struct. 28*, 1−27.
7. Overman, S. A., Tsuboi, M., and Thomas, G. J., Jr. (1996) *J. Mol. Biol. 259*, 331−336.
8. Tsuboi, M., Overman, S. A., and Thomas G. J., Jr. (1996) *Biochemistry 35*, 10403−10410.
9. Takeuchi, H., Matsuno, M., Overman, S. A., and Thomas, G. J., Jr. (1996) *J. Am. Chem. Soc. 118*, 3498−3507.

10. Matsuno, M., Takeuchi, H., Overman, S. A., and Thomas, G. J., Jr. (1997) *Biophys. J. 74*, 3217−3225.
11. Wen, Z. Q., and Thomas, G. J., Jr. (1998) *Biopolymers 45*, 247−256.
12. Wen, Z. Q., Overman, S. A., and Thomas, G. J., Jr. (1997) *Biochemistry 36*, 7810−7820.
13. Wen, Z. Q., Armstrong, A., and Thomas, G. J., Jr. (1999) *Biochemistry 38*, 3148−3156.
14. Austin, J., Jordan, T., and Spiro, T. G. (1993) in *Advances in Spectroscopy* (Clark, R. J. H., and Hester, R. E., Eds.) Vol. 20A, pp 55−127, John Wiley and Sons, New York.
15. Thomas, G. J., Jr., Prescott, B., and Day, L. A. (1983) *J. Mol. Biol. 165*, 321−356.
16. Russell, M. P., Vohník, S., and Thomas, G. J., Jr. (1995) *Biophys. J. 68*, 1607−1612.
17. Overman, S. A., Aubrey, K. L., Vispo, N. S., Cesareni, G., and Thomas, G. J., Jr. (1994) *Biochemistry 33*, 1037−1042.
18. Overman, S. A., and Thomas, G. J., Jr. (1995) *Biochemistry 34*, 5440−5451.
19. Overman, S. A., and Thomas, G. J., Jr. (1998) *Biochemistry 37*, 5654−5665.
20. Overman, S. A., and Thomas, G. J., Jr. (1999) *Biochemistry 38*, 4018−4027.
21. Harada, I., and Takeuchi, H. (1986) in *Spectroscopy of Biological Systems* (Clark, R. J. H., and Hester, R. E., Eds.) Vol. 13, pp 113−175, John Wiley and Sons, New York.
22. Almeida, F. C. L., and Opella, S. J. (1997) *J. Mol. Biol. 270*, 481−495.
23. Miura, T., Takeuchi, H., and Harada, I. (1988) *Biochemistry 27*, 88−94.
24. Miura, T., Takeuchi, H., and Harada, I. (1989) *J. Raman Spectrosc. 20*, 667−671.
25. Aubrey, K. L., and Thomas, G. J., Jr. (1991) *Biophys. J. 60*, 1337−1349.
26. Lakowicz, J. R. (1983) *Principles of Fluorescence Spectroscopy*, Plenum, New York.
27. Takeuchi, H., and Harada, I. (1986) *Spectrochim. Acta 42A*, 1069−1078.
28. Clark, P. L., Liu, Z. P., Zhang, J. H., and Gierasch, L. M. (1996) *Protein Sci. 5*, 1108−1117.
29. Markley, J. L., Bax, A., Arata, Y., Hilbers, C. W., Kaptein, R., Sykes, B. D., Wright, P. E., and Wüthrich, K. (1998) *J. Mol. Biol. 280*, 933−952.
30. Ponder, J. W., and Richards, F. M. (1987) *J. Mol. Biol. 193*, 775−791.
31. Miura, T., Takeuchi, H., and Harada, I. (1993) *FEBS Lett. 307*, 181−184.
32. Chi, Z., and Asher, S. A. (1998) *Biochemistry 37*, 2865−2872.
33. Dougherty, A. D. (1996) *Science 271*, 163−168.
34. Kleywegt, G. J., Bergfors, T., Senn, H., Motte, P. L., Gsell, B., Shudo, K., and Jones, T. A. (1994) *Structure 2*, 1241−1258.
35. McFail-Isom, L., Shui, X., and Williams, L. D. (1998) *Biochemistry 37*, 17105−17111.
36. Ma, J. C., and Dougherty, A. D. (1997) *Chem. Rev. 97*, 1303−1324.
37. Cubero, E., Luque, F. J., and Orozco, M. (1998) *Proc. Natl. Acad. Sci. U.S.A. 95*, 5976−5980.
38. Juszczak, L. J., Zhang, Z. Y., Wu, L., Gottfried, D. S., and Eads, D. D. (1997) *Biochemistry 36*, 2227−2236.
39. Schubert, H. L., Fauman, E. B., Stuckey, J. A., Dixon, J. E., and Saper, M. A. (1995) *Protein Sci. 4*, 1904−1913.
40. Stuckey, J. A., Schubert, H. L., Fauman, E. B., Zhang, Z., Dixon, J. E., and Saper, M. A. (1994) *Nature 370*, 571−575.
41. Marvin, D. A., and Wachtel, E. J. (1976) *Philos. Trans. R. Soc. London, Ser. B 276*, 81−98.
42. Marvin, D. A. (1990) *Int. J. Biol. Macromol. 12*, 125−138.
43. Thomas, G. J., Jr., and Day, L. A. (1981) *Proc. Natl. Acad. Sci. U.S.A. 78*, 2962−2966.
44. Marvin, D. A., Hale, R. D., Nave, C., and Citterich, M. H. (1994) *J. Mol. Biol. 235*, 260−286.
45. Karlin, S., Zuker, M., and Brocchieri, L. (1994) *J. Mol. Biol. 239*, 227−248.
46. Loewenthal, R., Sancho, J., and Fersht, A. R. (1991) *Biochemistry 30*, 6775−6779.

BI992018W